Fusion Engineering and Design 88 (2013) 2865–2869

Contents lists available at ScienceDirect

Fusion Engineering and Design

journal homepage: www.elsevier.com/locate/fusengdes

First results with the upgraded TLK tritium calorimeter IGC-V0.5

A. Bükki-Deme[a,*], C.G. Alecu[b], B. Kloppe[b], B. Bornschein[b]

[a] Institute for Nuclear Research, Hungarian Academy of Sciences (MTA Atomki), P.O. Box 51, H-4001 Debrecen, Hungary
[b] Karlsruhe Institute of Technology, Tritium Laboratory (TLK), P.O. Box 3640, D-76021 Karlsruhe, Germany

HIGHLIGHTS

- We have upgraded a 12 years old tritium calorimeter.
- We have developed a new control and data acquisition software using LabView.
- The retuned PID control loops increased stability and accuracy.
- The automatic control algorithm can reduce measurement time and avoid possible operator errors.
- We compared calibration results made with the original and the upgraded system.

ARTICLE INFO

Article history:
Received 22 January 2013
Received in revised form 2 April 2013
Accepted 20 May 2013
Available online 14 June 2013

Keywords:
Isothermal calorimetry
Tritium calorimetry
Inertial guidance vacuum calorimeter

ABSTRACT

At Tritium Laboratory Karlsruhe (TLK) calorimetry has been used for almost 20 years as the main accountancy method for tritium inventory. An extensive work has been carried out in order to improve the existing calorimeters. This paper covers the efforts made for the upgrade of the IGC-V0.5 calorimeter. We replaced the hardware interface – including the obsolete PC – and developed a new control and data acquisition software. The new software applies a smart automatic process control during measurements, significantly reducing measurement time and possible user errors. The three PID control loops have been re-tuned using the standard closed loop Ziegler–Nichols procedure to find the optimal PID parameters. Five calibration runs have been performed between 0.5 μW and 1 W, and their results are being presented and discussed.

1. Introduction

In a nuclear facility using tritium, it is of an extreme importance to have an adequate method for tritium accountancy. At TLK, calorimetry is the method being used for accountancy since 1993 [1]. Tritium has an unstable nucleus which decays into a stable He^3 nucleus, an electron and an antineutrino. The thermal heat produced by decay can be measured by calorimetry. 1 g of pure tritium has an activity of 358 TBq and produces 324 ± 0.9 mW heat [2]. Since this technique directly measures the decay heat, the sample can be in any physical form. This is the main advantage over other tritium analytics, we can even measure decay heat produced by entrapped tritium in solid bulk structural materials. The main disadvantages are the rather long measurement time (large volume means high heat capacity which results in large time constants of days), and the correlated long time instrumental noise in case of large volume samples. Depending on the required application, there are different calorimeters for tritium or other heat producer isotope measurements. When applications require short measurement time, there is a compromise in volume or sensitivity. Very precise twin isothermal calorimeters are available from the market, with μW detection limit, but their sample holder size is very limited, only up to a few ml. Industrially available, from-the-shelf large volume tritium calorimeters usually can not work below the mW range, but they are capable to do measurements on large volumes (even up to 70–80 l) in a relatively short time (<1 day). There are two companies, Setaram (France) and ANTECH (US), who sell large volume dedicated tritium calorimeters [3,4]. Song et al. report test results after deploying one of these large volume calorimeters [5]. Matsuyama et al. presented an isothermal twin calorimeter with outstanding lower detection limit (40 MBq) for tritiated water samples, however the sample volume is small: 24 ml [6]. Besides room temperature isothermal calorimeters, there are also more exotic methods for decay heat measurements, like cryogenic microcalorimeters. Colle and Zimmerman reported a device with μW measurement capability, on small volume samples [7].

Currently, TLK operates four calorimeters for accountancy, waste management and tritium inventory measurements in different samples [8]. One of them is the IGC-V0.5 inertial guidance vacuum calorimeter with 500 ml useful sample volume. Another

* Corresponding author. Tel.: +4915125506498.
E-mail addresses: bukkideme@atomki.hu, bukkideme@gmail.com (A. Bükki-Deme), catalin-gabriel.alecu@kit.edu (C.G. Alecu), beate.kloppe@kit.edu (B. Kloppe), beate.bornschein@kit.edu (B. Bornschein).

0920-3796/$ – see front matter © 2013 Elsevier B.V. All rights reserved.
http://dx.doi.org/10.1016/j.fusengdes.2013.05.066

Fig. 1. IGC-V0.5 inertial guidance vacuum calorimeter.

calorimeter at TLK called IGC-V25 has a useful sample volume of 20 l, and uses a very similar working principle as the IGC-V0.5. The IGC-V0.5 calorimeter was deployed at TLK twelve years ago. Among the other calorimeters, the IGC-V0.5 was the most accurate device able to measure tritium samples with activity from 10^9 Bq to 10^{16} Bq (1 μW to 1 W). While the IGC-V0.5 was still one of the best in its category, it had untapped potential mainly due to its age. In the following we describe the original system, the upgrade procedure, and finally we compare calibration results between the old and the upgraded system.

2. Description of IGC-V0.5

The IGC-V0.5 inertial guidance vacuum calorimeter (Fig. 1) uses a special thermostat design, which can achieve three orders of magnitude better temperature stability (±30 nK) at the reference point of the calorimeter compared to conventional thermostats (±10–100 μK) [9,10].

The task of the instrument is to measure heat flow between the sample holder and the reference point, called calorimeter base. Thermoelectric sensors (several Peltier-modules in inverse mode, connected together electrically serial and thermally parallel to greatly increase sensitivity) give an electrical signal proportional to the temperature gradient between their two sides, so this signal is also proportional to the heat flow rate. Fig. 2 shows the main elements of the calorimeter located inside the vacuum chamber. This schematic is a cross section of the calorimeter body with cylindrical geometry. A double walled vacuum chamber with recirculated water loop surrounds the inner parts. High vacuum (10^{-5} mbar) with super insulation (several layers of heat radiation shields; not shown in the schematic) permits heat transfer almost exclusively through the thermoelectric sensors and the heat pumps. Additionally, the vacuum chamber is covered with Styrofoam insulation sheets from outside.

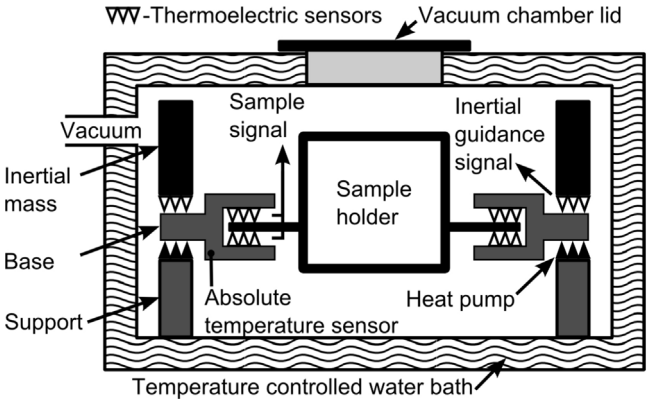

Fig. 2. Schematics of IGC-V0.5 inertial guidance vacuum calorimeter.

The temperature of the base must be appropriately stable, in order to get proper signal from the calorimeter sensors between the sample holder and the base. The instrument achieves its ultimate stability in three steps. First, the system starts to control the temperature of the recirculated water loop around the vacuum chamber (setpoint is 22.2 °C). A conventional absolute temperature sensor (ATS, PT100 platinum resistor) measures the temperature of the water, and a PID algorithm controls a thermoelectric water-to-air heat pump. Reaching the required temperature stability of the water loop, the coarse temperature control starts to stabilize the temperature of the base (its setpoint is 22.3 °C in order to create heat flow toward the water loop). This again uses conventional PT100 sensor and PID control to drive the heat pumps between the water loop and the base using a Keithley 2400 sourcemeter. When the temperature of the base in this coarse control becomes stable, the fine temperature control of the base has to be activated. This is done by freezing the output of the PID of the coarse control (the actual electrical current value of the Keithley 2400 is fixed). The process value of the fine control stage is the thermoelectric signal from sensors located between the base and the inertial (thermal) mass. Due to the high heat capacity of the inertial mass module, even small temperature fluctuations give measurable (Keithley 2182 nanovoltmeter) signals. This temperature derivative sensor signal (TDS, or inertial guidance signal) drives another Keithley 2400 sourcemeter through a PID algorithm. Theoretically a zero TDS signal indicates that there is no net heat flow between the inertial mass and the base, so the base is in thermal equilibrium. The output of the fine control loop is then electrically added to the fixed current of the coarse control loop. This combined electrical current drives the heat pump array between the base and the support. The TDS sensor has a sensitivity of 1.6 V/K, and the setpoint of this fine base control is −4.4 μV (non zero due to parasitic voltages). A more detailed description of an inertial guidance vacuum calorimeter can be found in [9,10].

3. New control system

The original control and data acquisition (DAQ) software was written in NI LabView 7.2 in 2004. A PC with PCI GPIB interface card gave the hardware part of the system. The PC communicated with the Keithley 2010 multimeters, 2400 sourcemeters, and the 2182 nanovoltmeter via the GPIB interface. Three simple and separated LabView programs (Virtual Instruments, VIs) drove the three stages of the calorimeter (water loop, coarse base loop, fine base loop). Another LabView VI was used for DAQ, and a fourth one was used for calibration sequence control. With this simple design, a full automatic control was not possible. The human operator had to make decisions when and how to start the different control stages of the device, increasing the possibility of mistakes.

3.1. Hardware changes

We replaced the old PC with a new one, and the system also got a new GPIB interface (NI GPIB-USB-HS) connecting all the Keithley instruments to the PC via USB. It was not possible to monitor room temperature during calibration runs before, because the same Keithley instrument (2010 multimeter) was also used to measure the voltage drop on the precision resistor connected serially to the calibration resistor. Therefore, we purchased a NI USB-TC01 cold junction compensated thermocouple to continuously and independently monitor room temperature even during calibrations.

3.2. New control and DAQ software

The new software was written using LabView 2011, including the latest VISA (Virtual Instrument Software Architecture) drivers for the Keithley instruments and the USB-TC01 temperature sensor. The new software is a compact VI, including different modules to PID control the stages of the calorimeter, collect and statistically analyze sensor data, and also logging the results in NI TDMS (technical data management streaming) files. The new software can work automatically and does not require any user interaction. The software first starts to control the temperature of the water loop. When the temperature stability of the water loop reaches a pre-defined value, the software shifts the system into the second stage: the coarse temperature control of the base is initiated. When the system reaches the ultimate stability of this coarse control loop, the software stops it, and the third stage, the fine control loop initiates. It is very important to ensure that the fine control loop only starts when the ultimate stability of the coarse control loop is reached and the temperature of the inertial mass module is very close to the temperature of the base. This was a weak point in the old system: the human operator had to wait long enough to be sure about the above conditions are fulfilled before freezing the coarse control and starting the fine one. If the operator only checked the stability of the base absolute temperature to make the decision for starting the fine control, this might have been too early: if the temperature of the inertial mass structural element is not enough close to the base yet, the coarse control might be stopped at an inappropriate electrical current output value. After some time, the electrical current requisite for the heat pumps can change as the temperature of the inertial mass changes. Because the fine control can work only in the ±1 mA range (coarse control loop uses the ±100 mA current range for the Keithley 2400), there will be no spare current to compensate this effect. Therefore, the operator had to go back to the coarse control stage when the old, original system was used. On the other hand, the operator could wait too long to reach the coarse control equilibrium. This situation is neither favorable since it would significantly increase the measurement time.

The new system must automatically shift from the coarse control to the fine one at the optimal moment. The software monitors the TDS fine signal already during the coarse control (ATS). The transition only happens, when the ATS signal is stable and the TDS signal indicates that the inertial mass is equilibrated to the temperature of the base, so there is no significant drift in the TDS signal (see flow chart in Fig. 3). The improvement in the measurement time practically comes from the fact, that the new system does not need the operator's interaction to switch from coarse to fine control. During sample holder replacements we ventilate the vacuum system. The calorimeter needs approximately 12 h in coarse mode to be ready to switch again to the fine control state. If the operator ventilates the system in the afternoon, the new automatic software will produce the result (baseline or sample signal level) by the morning (the inspected zone of the laboratory is closed between 6 pm and 7 am). With the old software, the operator had the chance to switch to fine control state only in the morning. So the improvement is about half day for one ventilation procedure. One measurement requires two ventilations if we start with a stable baseline (baseline-sample signal-baseline).

The temperature stability of the different zones has the largest impact on the achievable stability of the calorimeter signal. Therefore, the key modification was to properly tune the three control loops during the upgrade of the calorimeter. We used the standard closed-loop Ziegler–Nichols PID tuning protocol [11], to find the optimal PID parameters. The stability significantly increased: while the standard deviation of the calorimeter signal was in the range of the 10^{-7} V, now it is in the range of the 10^{-8} V.

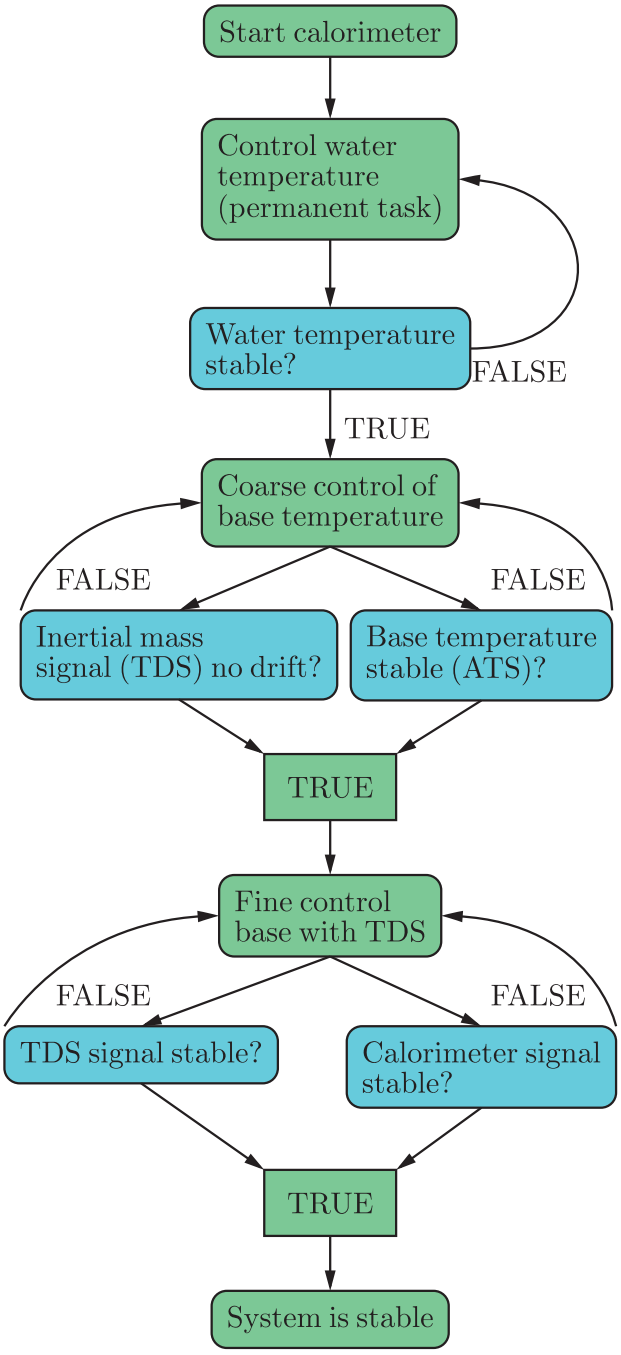

Fig. 3. Flowchart of the new control software.

4. Calorimetric measurement

First, a base line measurement is recorded. The base line is the reference voltage which can be measured on the calorimeter sensors when the sample holder is empty. Afterwards, the sample measurement takes places. Finally, a new measurement of the base line is made. This measurement can later be used as the initial base line for a new sample to be measured. Also the room temperature is being recorded during all three measurements. It has been observed that the temperature variation has the highest impact on the stability of the calorimeter.

The results of the two base lines, U_{BL1} and U_{BL2}, are compared in order to check for the calorimeter stability. If the difference between the two base lines, δU_{BL}, is within a certain range then the

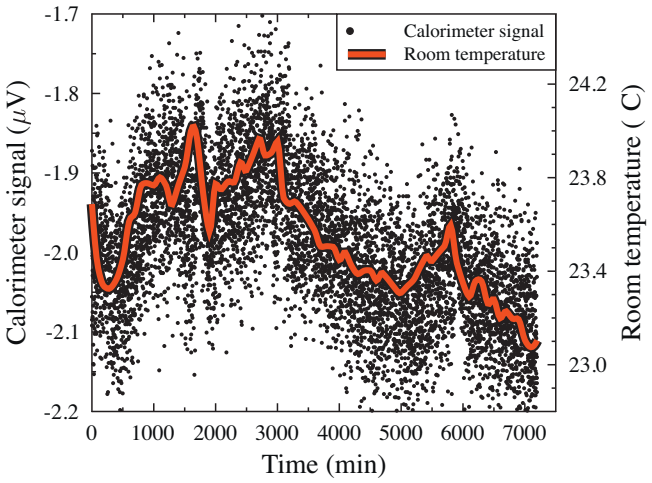

Fig. 4. Scatter plot of the raw calorimeter signal over a five day long measurement. Room temperature was recorded simultaneously.

measurement is validated. Otherwise the complete measurement has to be repeated. Obviously it is also mandatory that the value of the sample signal, ΔU, is large enough to differentiate between the uncertainty of the average base line and of the sample measurement. At TLK, for samples below 10^{-4} W the measurement is validated only if the difference between the values of the base lines, δU_{BL}, is less than 20% of the value of the sample, ΔU.

5. Performance assessment after upgrade

The performance was investigated through the calorimeter signal stability and the accuracy determined by calibration.

5.1. Signal stability

The main source of the noise in the calorimeter signal is the PID fine control of the base temperature. The second largest impact on the signal stability is the variation of the room temperature. Room temperature fluctuations do not cause problems up to a certain level: the effect of the temperature variations below this level is negligible compared to the noise introduced by the base fine control. However, above this level the room temperature fluctuation will rule the long term stability of the calorimeter signal. This effect is presented in Fig. 4. One can see the constant level of the noise is ~0.3 μV. If the room temperature varies with an amplitude higher than ~0.5 °C, the calorimeter signal deviation will be larger than the noise level. Note that only long term room temperature changes (more than 1 h) can affect the calorimeter signal. Obviously, sudden room temperature fluctuations are depleted due to the high heat capacity of the calorimeter thermal shield (water jacket and Styrofoam insulation).

5.2. Calorimeter calibration

In order to calibrate the calorimeter we used the Joule-effect method. The calibration setup and procedure are presented in [12]. We ran five calibration sequences using the automatic calibration algorithm of the new LabView software. Each calibration run covered the whole power range from 0.5 μW to 1 W. In order to be more accurate, for the calculation of the calibration power, P_{cal}, we have used the value U_{cal}, measured across the calibration resistor and not the resistivity value of the calibration resistor, R_{cal}. Therefore:

$$P_{cal} = U_{cal} \cdot \left(\frac{U_1}{R_1}\right) \tag{1}$$

where U_1 represents the value of the voltage drop across the 1 Ω certified precision resistor R_1 ($R_1 \ll R_{cal}$) used to determine the calibration current, I_{cal} (R_{cal} and R_1 connected in serial). For each measurement, a calibration factor, $CF^{(P)}$, was determined as a ratio between the calibration power, P_{cal}, and the calorimeter signal, ΔU:

$$CF^{(P)} = \frac{P_{cal}}{\Delta U} \tag{2}$$

For a complete calibration series, a global calibration factor, CF, was determined using linear regression method for the whole covered power range:

$$CF = a + b \cdot P \tag{3}$$

where a represents the theoretical value of the calibration factor at 0 W and b represents the slope of the calibration curve. Using Eqs. (2) and (3) one can determine the power of a certain sample using the calorimeter signal, ΔU, and the calibration parameters, a and b:

$$P = \frac{a \cdot \Delta U}{1 - b \cdot \Delta U} \tag{4}$$

5.3. Calorimeter accuracy

In the actual work, the focus was on the determination of the calorimeter's accuracy over the whole calibration range. First, the uncertainty of the sample signal has to be determined using the uncertainty of the measurement, δ_U, and the overall uncertainty of the base line, δ_{BL}, determined for the average value of the base line, U_{BL}. These uncertainties are determined as the standard deviation of the last hour of measurement (3600 samples), when the calorimeter signal is stable. The sample signal uncertainty, $\delta_{\Delta U}$ is:

$$\delta_{\Delta U} = \sqrt{(\delta_U)^2 + (\delta_{BL})^2} \tag{5}$$

The uncertainty of the calibration power, δP_{cal}, takes into account the uncertainties of the voltage drops across the calibration resistor, δU_{cal}, across the certified resistor, δU_1, and also the uncertainty of the certified resistor, δR_1:

$$\delta P_{cal} = P_{cal} \cdot \sqrt{\left(\frac{\delta U_{cal}}{U_{cal}}\right)^2 + \left(\frac{\delta U_1}{U_1}\right)^2 + \left(\frac{\delta R_1}{R_1}\right)^2} \tag{6}$$

The uncertainty of the calibration factor for a certain calibration power, $\delta_{CF}^{(P)}$, is determined by taking into consideration the uncertainty of the sample signal, $\delta_{\Delta U}$, the uncertainty of the calibration power, δP_{cal}, and also the absolute difference between the calculated calibration factor, $CF^{(P)}$, and the fitted calibration factor, CF:

$$\delta_{CF}^{(P)} = CF^{(P)} \cdot \sqrt{\left(\frac{\delta P_{cal}}{P_{cal}}\right)^2 + \left(\frac{\delta_{\Delta U}}{\Delta U}\right)^2 + |CF^{(P)} - CF|} \tag{7}$$

The uncertainty of the sample power at a certain calibration power, $\delta P^{(P)}$, can be determined by taking into consideration the uncertainty of the calibration factor at that power, $\delta_{CF}^{(P)}$, and the uncertainty of the sample signal, $\delta_{\Delta U}$:

$$\delta P^{(P)} = P \cdot \sqrt{\left(\frac{\delta_{CF}^{(P)}}{CF^{(P)}}\right)^2 + \left(\frac{\delta_{\Delta U}}{\Delta U}\right)^2} \tag{8}$$

It has been observed that the uncertainty of the sample power, which represents the accuracy of the calorimeter, increases as the sample power increases. Using the linear regression method it was possible to determine the accuracy curve. This curve establishes

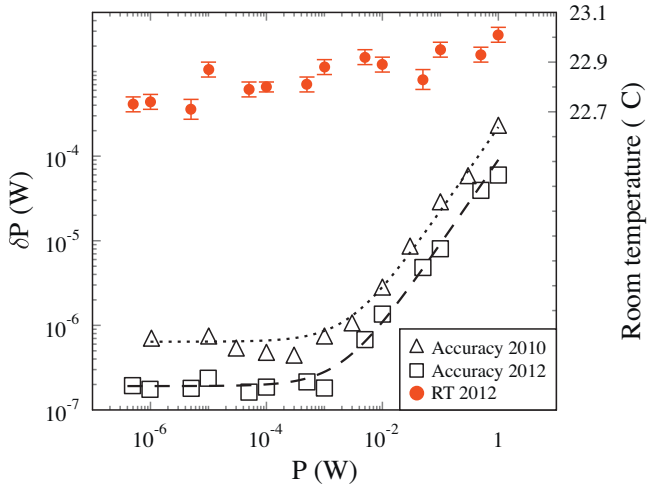

Fig. 5. Comparing calibration results from 2010 and 2012. Room temperature data also included for the case 2012.

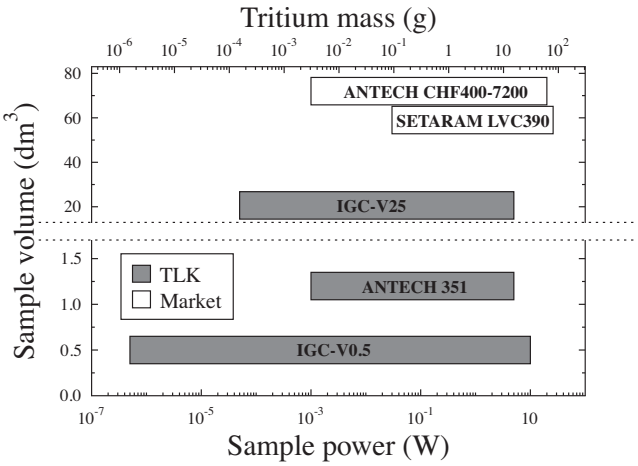

Fig. 6. Recently available tritium calorimeters at TLK and two large volume calorimeters from the market (ANTECH 351 is a commercial power compensation tritium calorimeter from the 1990s).

the relation between the accuracy of the calorimeter, δP, and the sample power, P:

$$\delta P = a_P + b_P \cdot P \quad (9)$$

where a_P represents the minimum reachable accuracy (at 0 W) and b_P represents the slope of the accuracy curve.

In Fig. 5, we present the comparison between the calibrations ran in 2010 (original system) and 2012 (upgraded system).

One can easily see that there is a significant increase in accuracy, specially at lower powers. Moreover, the detection limit has been decreased from 1 μW (2010) to 0.5 μW (2012).

The new system allows the room temperature to be recorded even during calibration (using the new USB-TC01 temperature sensor), also shown in Fig. 5. During the 2012 calibration sequence, the room temperature variation was smaller than 0.3 °C, ensuring that the room temperature had no significant effect on the results.

6. Conclusion

We significantly increased the accuracy of the IGC-V0.5 calorimeter, especially for the low power range. At 1 μW, the relative accuracy has been improved from 60% to 17%. In terms of mass, now we are able to measure samples containing 1.5 μg tritium with an accuracy of ±0.5 μg (~500 ± 166 MBq). Besides, the new software reduces measurement time and avoids possible human operator errors. Finally, we compare three calorimeters recently owned by TLK and two which are available from the market (Fig. 6, the performance of the IGC-V0.5 is post-upgrade). Note that this comparison (specification data is taken from company websites) does not include info about measurement time, which is much shorter in the case of the commercial calorimeters.

Acknowledgments

We would like to thank J.L. Hemmerich for the useful discussions.

This work, supported by the European Communities under the contract of Association between EURATOM/ATOMKI, was carried out within the framework of the "Tritium Technologies for the Fusion Fuel Cycle" (Task Agreement no. WP08-GOT-TRI-TOFFY). The views and opinions expressed herein do not necessarily reflect those of the European Commission.

References

[1] R.-D. Penzhorn, N. Bekris, P. Coad, L. Dörr, M. Friedrich, M. Glugla, et al., Status and research progress at the Tritium Laboratory Karlsruhe, Fusion Engineering and Design 49-50 (2000) 753–767.
[2] P.C. Souers, Hydrogen Properties for Fusion Energy, University of California Press, Berkley/Los Angeles, CA, 1986, pp. 208.
[3] http://www.setaram.com
[4] http://www.antech-inc.com
[5] K.-M. Song, K.-M. Song, B.-W. Ko, K.-W. Lee, S.-H. Sohn, Test of a large-volume calorimeter in KEPRI Tritium Laboratory, IEEE Transactions on Plasma Science 38 (2010) 295–299.
[6] M. Matsuyama, K. Takatsuka, M. Hara, Sensitivity of a specially designed calorimeter for absolute evaluation of tritium concentration in water, Fusion Engineering and Design 85 (2010) 2045–2048.
[7] R. Collé, B.E. Zimmerman, A dual-compensated cryogenic microcalorimeter for radioactivity standardizations, Applied Radiation and Isotopes 56 (2002) 223–230.
[8] L. Dorr, U. Besserer, S. Grunhagen, M. Glugla, B. Kloppe, M. Sirch, et al., High resolution vacuum calorimeter, Fusion Science and Technology 48 (2005) 358–361.
[9] J.L. Hemmerich, L. Serio, P. Milverton, High-resolution tritium calorimetry based on inertial temperature control, Review of Scientific Instruments 65 (1994) 1616.
[10] J.L. Hemmerich, J.-C. Loos, A. Miller, Advances in temperature derivative control and calorimetry, Review of Scientific Instruments 67 (1996) 3877.
[11] J. Ziegler, N. Nichols, Optimum settings for automatic controllers, Journal of Dynamic Systems, Measurement, and Control 115 (1993) 220–222.
[12] C.G. Alecu, U. Besserer, B. Bornschein, B. Kloppe, Z. Köllő, J. Wendel, Reachable accuracy and precision for tritium measurements by calorimetry at TLK, Fusion Science and Technology 60 (2011) 937–940.